The influence of fluorine position on the properties of fluorobenzoxaboroles

ARTICLE *in* BIOORGANIC CHEMISTRY · MAY 2015

Impact Factor: 2.15 · DOI: 10.1016/j.bioorg.2015.05.004

12 AUTHORS, INCLUDING:

Agnieszka Adamczyk-Woźniak

Warsaw University of Technology

34 PUBLICATIONS **246** CITATIONS

SEE PROFILE

Jacek Lipok

Opole University

31 PUBLICATIONS **174** CITATIONS

SEE PROFILE

Lukasz Popenda

Adam Mickiewicz University

20 PUBLICATIONS **51** CITATIONS

SEE PROFILE

Grzegorz Schroeder

Adam Mickiewicz University

390 PUBLICATIONS **3,405** CITATIONS

SEE PROFILE

Bioorganic Chemistry 60 (2015) 130–135

Contents lists available at ScienceDirect

Bioorganic Chemistry

journal homepage: www.elsevier.com/locate/bioorg

The influence of fluorine position on the properties of fluorobenzoxaboroles

Agnieszka Adamczyk-Woźniak [a], Małgorzata K. Cabaj [b], Paulina M. Dominiak [b], Patrycja Gajowiec [a], Błażej Gierczyk [c], Jacek Lipok [d], Łukasz Popenda [e], Grzegorz Schroeder [c], Ewelina Tomecka [a], Piotr Urbański [a], Dorota Wieczorek [d], Andrzej Sporzyński [a,*]

[a] Faculty of Chemistry, Warsaw University of Technology, Noakowskiego 3, 00-664 Warsaw, Poland
[b] Faculty of Chemistry, University of Warsaw, Pasteura 1, 02-093 Warsaw, Poland
[c] Faculty of Chemistry, Adam Mickiewicz University in Poznań, Umultowska 89b, 61-614 Poznań, Poland
[d] Faculty of Chemistry, Opole University, Oleska 48, 45-052 Opole, Poland
[e] NanoBioMedical Centre, Adam Mickiewicz University in Poznań, Umultowska 85, 61-614 Poznań, Poland

ARTICLE INFO

Article history:
Received 4 March 2015
Available online 14 May 2015

Keywords:
Benzoxaboroles
Tavaborole
Antifungal activity
Crystal structure

ABSTRACT

5-Fluoro-2,1-benzoxaborol-1(3H)-ol, a potent antifungal drug also known as Tavaborole or AN2690, has been compared with its three isomers in terms of its activity against several fungi as well as pK_a and multinuclear NMR characterization. The molecular and crystal structure of 6-fluoro-2,1-benzoxaborol-1(3H)-ol was determined and compared with that of AN2690.

1. Introduction

Benzoxaboroles are important organoboron compounds due to their specific properties and wide applications. The benzoxaborole structural motif has been applied for medicinal purposes [1] such as HIV entry inhibitors [2–4], antiprotozoal drugs [5], antibacterial or antifungal agents [6,7] as well as a potential drug delivery scaffold [8]. Their applications in biotechnology and therapeutic treatments was recently reviewed [9].

5-Fluoro-substituted benzoxaborole (**1**, Chart 1), is a FDA-approved drug KERYDIN™ (Tavaborole), the first oxaborole antifungal dedicated for the topical treatment of onychomycosis of the toenails [10]. The mechanism of its antifungal activity is based on the interaction with the active site of enzyme, which results in inhibition of LeuRS and blocking the protein synthesis [11,12]. The history of these investigations and mechanism of action have been recently described [9].

Our recent research on the structures and properties of organoboron compounds was focused on the characterization of fluoro-substituted phenylboronic compounds. Generally, introduction of fluorine atoms increases the acidic character of the boronic center. It was found that cyclic boronic esters with fluorine atom at the *ortho* position display higher acidity in comparison with other monosubstituted isomers. Increasing the number of fluorine substituents does not simply result in rise of the acceptor number for these compounds [13], and the overall Lewis acidity of equally fluorinated diol phenylboronates is significantly affected by the structure of the diol [14]. The number and position of the fluorine substituents has also a substantial influence on the crystal structure of phenylboronates [15]. In case of fluorinated acids, introduction of *ortho*-fluorine atom weakens the intermolecular hydrogen bond [16,17]. Moreover, results of the systematic NMR studies of fluorinated phenylboronic acids revealed a close correlation between their structure and spectroscopic properties [18].

Tomsho et al. [19] showed that the substituents in benzene ring of benzoxaboroles follow a Hammett relationship with the pK_a values. Moreover, these substituents' effects are also related to the polyols binding properties of these compounds under physiologically relevant conditions. The presence of fluorine substituent as well as its position are crucial from the point of view of the antifungal activity [20,21].

The compounds under investigation are four isomeric benzoxaboroles with fluorine substituent in benzene ring at various positions. The aim of this work is to compare their properties:

* Corresponding author. Fax: +48 22 6282741.
E-mail address: spor@ch.pw.edu.pl (A. Sporzyński).

http://dx.doi.org/10.1016/j.bioorg.2015.05.004
0045-2068/

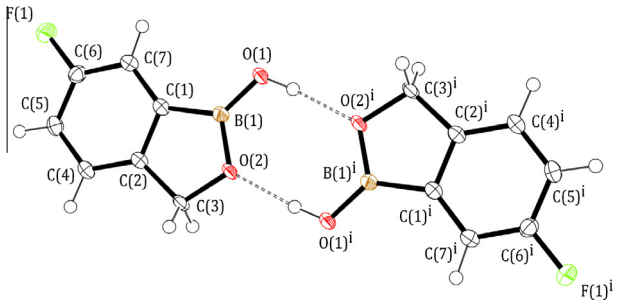

Fig. 1. Molecular structure of **2** from single crystal X-ray diffraction (XRD) data. Ellipsoids corresponding to anisotropic thermal displacement parameters (ADP's) drawn at the 50% probability level. Hydrogen atoms (refined isotropically) are shown with an arbitrary radius. Second molecule (labels with superscript *i*) generated by $1 - x$, $-y$, $1 - z$ symmetry operation.

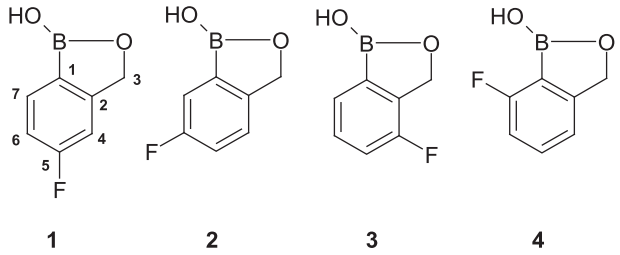

Chart 1. Benzoxaboroles under investigation.

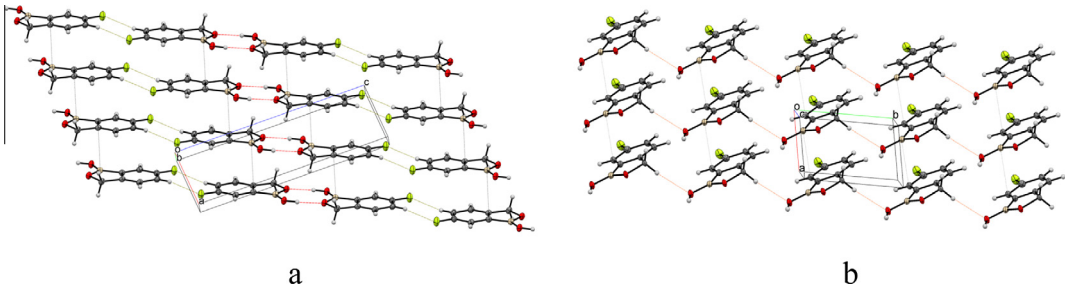

Fig. 2. Crystal packing pattern in the solid-state structure of **2**: along the *b*-axis with the O–H···O hydrogen bonds and C–H···F interactions (a), along the *c*-axis with the C–H···O interactions (b).

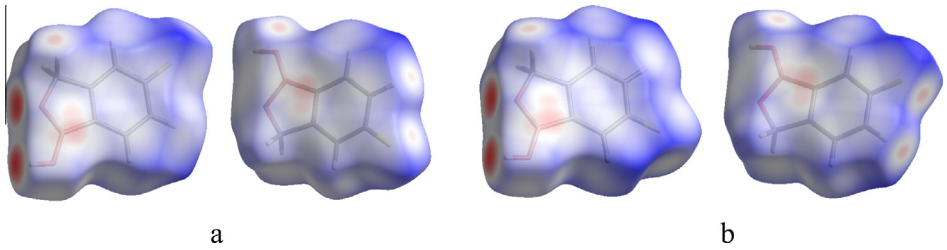

Fig. 3. Visualization of Hirshfeld surface attributed to **1** (a) and **2** (b) solid-state structures; the shortest contacts in the crystal bulk (colored red) are associated with hydrogen bonds (strong O–H···O, weak C–H···F and C–H···O), wherein interactions perpendicular to molecule plane may be ascribed to weak $\pi\cdots\pi$ stacking interactions.

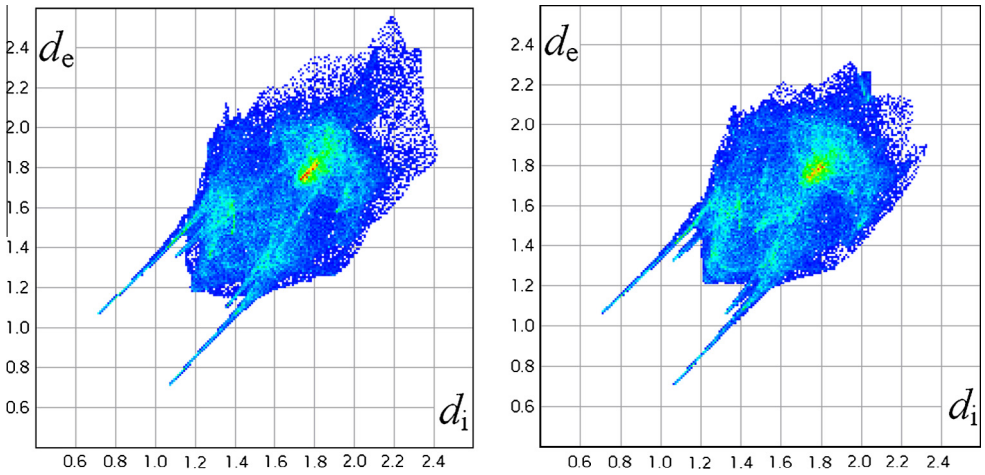

Fig. 4. Two-dimensional fingerprint plot attributed to **1** (left) and **2** (right) solid-state structures, presenting combination of distances external (d_e, in Å) and internal (d_i, in Å) to the Hirshfeld surface; the shortest contacts in the crystal bulk are associated with O–H···O and C–H···F hydrogen bonds (indicated by pairs of long sharp spikes).

structural and spectral parameters, acidity as well as antifungal activity.

Table 1
Comparison of key bond lengths (Å) and angles (°) of the compounds **1** and **2**.

Bond/angle	**1** (Ref. [22])	**2**
F1–C5/C6	1.3562(15)	1.3634(19)
O1–B1	1.3483(18)	1.351(2)
O2–C2	1.4471(15)	1.4518(18)
O2–B1	1.3922(17)	1.395(2)
C1–B1	1.5522(18)	1.552(2)
O1–H1···O2	2.7614(13)	2.7572(16)
O1–B1–O2	121.51(12)	121.48(15)
O1–B1–C1	130.25(12)	130.09(15)
O2–B1–C1	108.24(11)	108.43(13)

Table 2
pK_a values for the investigated compounds at 25.0 °C.

1[a]	**2**[b]	**3**[c]	**4**
6.97 ± 0.02	6.57 ± 0.08	6.36 ± 0.04	7.42 ± 0.15

[a] The value ca. 6.7 is given in the review paper [21], but the source of this data is not specified.
[b] Ref. [19]: 6.63.
[c] Ref. [19]: 6.45.

2. Results and discussion

The compounds investigated in the present paper with numbering of carbon atoms are shown in Chart 1.

2.1. Structures

Molecular and crystal structure of **1** was described previously [22]. Recently, extensive investigation on the structure and spectral properties of this compound was performed [23]. Determination of the crystal structure is important in the rational design of drug-like molecules [24], therefore we decided to study the influence of fluorine position on crystal structure of fluorobenzoxaboroles The present paper describes molecular structure of 6-fluoro-2,1-benzoxaborol-1(3*H*)-ol (**2**), Fig. 1.

Crystal data and other parameters related to data collection are summarized in Supplementary material: crystal data and structural refinement (Table S1), refined geometric parameters (Table S2), hydrogen-bond data (Table S3), atomic coordinates and thermal displacement parameters (Table S4), and described in experimental section. Selected data for the compounds **1** and **2** are collected in Table 1.

In the solid-state structure of both **1** [22] and **2** the planar $C_7H_6BFO_2$ molecules form centrosymmetric dimers due to strong O–H···O hydrogen bonds, wherein the dimers are arranged into layers by weak intermolecular C–H···F (Fig. 2a) and C–H···O

Table 3
NMR data (δ/ppm, J/Hz) for the investigated compounds (in $[^2H]_3$-acetone; 298 K).

	1	**2**	**3**	**4**
^1H				
BOH	8.2; bs	8.4; bs	8.37; s	8.23; s
H3	5.02; s	5.00; s	5.10; s	5.04; t $^4J_{H3H4} = {}^6J_{H3H6} = 0.8$
H4	7.19; ddq $^3J_{H4F5} = 9.4$ $^4J_{H4H6} = 2.3$ $^5J_{H4H7} = {}^4J_{H4H3} = 0.7$	7.43; ddq $^3J_{H4H5} = 8.3$ $^4J_{H4F6} = 4.6$ $^5J_{H4H7} = {}^4J_{H4H3} = 0.9$	–	7.24; ddq $^3J_{H4H5} = 7.4$ $^5J_{H4F7} = 1.6$ $^4J_{H4H6} = {}^4J_{H3H4} = 0.8$
H5	–	7.23; ddd $^3J_{H5F6} = 9.4$ $^3J_{H4H5} = 8.3$ $^4J_{H5H7} = 2.6$	7.19; ddd $^3J_{F4H5} = 9.7$ $^3J_{H5H6} = 7.9$ $^4J_{H5H7} = 0.8$	7.53; ddd $^3J_{H5H6} = 8.1$ $^3J_{H4H5} = 7.4$ $^4J_{H5F7} = 5.3$
H6	7.11; dddt $^3J_{H6F5} = 9.4$ $^3J_{H6H7} = 8.0$ $^4J_{H4H6} = 2.3$ $^6J_{H6H3} = 0.8$	–	7.41; dddt $^3J_{H5H6} = 7.9$ $^3J_{H6H7} = 7.2$ $^4J_{F4H6} = 4.4$ $^6J_{H3H6} = 0.8$	7.00; tq $^3J_{H5H6} = {}^3J_{H6F7} = 8.1$ $^4J_{H4H6} = {}^6J_{H3H6} = 0.8$
^{13}C				
C1	127.3; b	133.9; b	136.4; b	119.1; b
C2	158.14; d $^3J_{CF} = 8.8$	150.68; d $^4J_{CF} = 1.5$	141.21; d $^2J_{CF} = 14.9$	159.38; d $^3J_{CF} = 8.8$
C3	70.86; d $^4J_{CF} = 3.1$	70.92	68.85	72.16
C4	109.16; d $^2J_{CF} = 22.1$	123.97; d $^3J_{CF} = 8.1$	158.91; d $^1J_{CF} = 247.5$	119.60; d $^4J_{CF} = 3.6$
C5	165.81; d $^1J_{CF} = 247.5$	116.61; d $^2J_{CF} = 20.2$	118.55; d $^2J_{CF} = 19.2$	135.67; d $^3J_{CF} = 7.4$
C6	115.34; d $^2J_{CF} = 22.2$	163.17; d $^1J_{CF} = 242.7$	131.37; d $^3J_{CF} = 5.6$	115.03; d $^2J_{CF} = 22.7$
C7	133.32; d $^3J_{CF} = 9.3$	118.80; d $^2J_{CF} = 23.6$	128.08; d $^4J_{CF} = 3.6$	166.32; d $^1J_{CF} = 250.1$
^{19}F				
	−111.84; td $^3J_{H4F5} = {}^3J_{H6F5} = 9.4$ $^4J_{H7F5} = 5.7$	−118.40; b	−121.46; ddd $^3J_{F4H5} = 9.7$ $^4J_{F4H6} = 4.4$ $^5J_{F4H7} = 1.2$	−105.51; ddd $^3J_{H6F7} = 8.1$ $^4J_{H5F7} = 5.3$ $^5J_{H4F7} = 1.6$
^{17}O				
BOH	66.3	67.2	68.0	68.3
BOC	99.1	100.9	96.3	97.5

(Fig. 2b) interactions, forming a two-dimensional supramolecular assembly which can be described by the layer group $p\bar{1}$. Interactions between parallel planar molecules are also observed. Weak B(sp^2)$\cdots\pi$ interactions between parallel molecules build up the three-dimensional structure. Supramolecular structures of both compounds in the solid state are very similar, which is confirmed by Hirshfeld surfaces [25,26] as well as by fingerprint plots [25,27] of these two compounds (Figs. 3 and 4). On the Hirshfeld surface (Fig. 3) red spots are indicators of intermolecular contacts with distances below the sum of the van der Waals radii of interacting atoms. On the two-dimensional fingerprint plots (Fig. 4), d_e is the distance from a point on the Hirshfeld surface to the nearest nucleus outside the surface, while d_i is the distance from a point on the surface to the nearest nucleus inside the surface. The shortest intermolecular distances are associated with strong O–H$\cdots$O hydrogen bond. Short contacts according to C–H$\cdots$F and C–H$\cdots$O hydrogen bonds and weak B(sp^2)$\cdots\pi$ and $\pi\cdots\pi$ interactions are also distinctly perceivable. Two-dimensional fingerprint plots features two pairs of long sharp spikes characteristic of a strong hydrogen bond, and a 'concentration' of contacts ca. 1.8 Å indicating significant contribution made by B(sp^2)$\cdots\pi$ and $\pi\cdots\pi$ interactions, wherein oxygen and hydrogen atoms, and also fluorine atoms, are involved in the shortest contacts.

2.2. pK_a values

One of the physicochemical properties crucial in the case of potential drugs is their pK_a, influencing such factors as solubility and bioavailability. The results of pK_a measurements are collected in Table 2.

As it was expected, compounds **1**, **2** and **3** display considerably lower pK_a value (higher acidity) in comparison with unsubstituted benzoxaborole (pK_a = 7.39) [28]. Surprisingly, compound **4** has a higher value, similar to that of fluorine-substituted phenylboronic acids [29]. Decrease of the acidity of boronic acids can be caused by the factors which make difficult the formation of the tetrahedral boronate ion. It was observed for phenylboronic acids with bulky substituents at *ortho* position [30]. In the case of benzoxaboroles, the likelihood of tetrahedral ion formation can be reduced by the formation of the rigid planar structure of the benzoxaborole molecule with additional intramolecular B–O–H$\cdots$F hydrogen bond, which is not possible for other isomers. The presence of such a bond in analogous 2-fluorophenylboronic acid was proved by X-ray in solid state [16] as well as by ^{19}F NMR in solution [18].

2.3. NMR spectroscopy

Chemical shifts and coupling constants for the investigated compounds are presented in Table 3. Numbering of carbon atoms in benzoxaborole molecules is shown in Chart 1. The studied compounds show distinct coupling of H-3 (methylene group) to H-4 and H-6 (1, 3) or H-4 only (2, 4). These couplings correspond to scalar spin–spin interaction via four or six bonds. They result in splitting of aromatic proton signal, they cause however only a broadening of H-3 peak. Only in 3 the CH_2 signal shows multiplicity. Coupling between H-3 and fluorine atom is not observed. Similarly to arylboronic acids, in the ^{13}C spectra of compounds studied the C-1 signal is difficult to observe, because of its huge broadening ($\Delta\nu_{1/2} \sim 200$–300 Hz) and low intensity. It is caused by the fast relaxation related to the proximity of the quadrupolar B-11 isotope. The effects of B(OH)OR substituent on C-1 chemical shifts are smaller than that for –B(OH)$_2$ group (+4.2 *vs.* +7.4 ppm, respectively, comparing with chemical shifts values for fluorobenzene). The chemical shifts of C-2 atoms are very characteristic. Their deshielding to over 140 ppm is caused by electronic effect of B atom at *ortho* position and strain effect of the five-membered ring fused to benzene one. Due to inductive effect of fluorine substituent the ^{17}O NMR chemical shift values for compounds **1**–**4** are slightly higher than that reported for the parent benzoxaborole (64.3 and 96.0 ppm for HO and BOC, respectively) [31]. The signals of BOH oxygen atoms are shielded by 7–14 ppm in comparison with parent fluorophenylboronic acid. This is the effect of increasing of C^1–B–O angle in benzoxaboroles, resulting in decreasing of steric interactions between oxygen BOH atom and aryl ring. The chemical shift of B–O–C oxygen atom is typical for esters of arylboronic acids.

2.4. Biological activity

Compounds **1** to **4** were studied in terms of their activity toward six fungal strains: *Aspergillus niger*, *Aspergillus terreus*, *Fusarium oxysporum*, *Fusarium solani*, *Penicillium ochrochloron*, and *Candida tenuis*. The strength of antifungal activity investigated by diffusion method in agar are collected in Table 4.

All of tested compounds showed inhibition activity on the growth of examined fungi. In previous work it was proved that the presence of fluorine atom in the structure of boronates is crucial for antimicrobial activity of these compounds [6,20]. The newly obtained results, confirm that not only the presence, but also the position of fluorine atom significantly influences this aspect. Hereby 5-fluoro-substituted benzoxaborole (**1**) revealed the highest activity against filamentous fungi. In the case of this compound, the diameters of the zone of totally inhibited growth of all tested molds, equaled to at least 62 mm (for 100 μg of boronate). However worth noting is that even half of this amount (50 μg) acted with similar efficiency, inhibiting totally the growth of tested mycelial fungi in the zone of at least 55 mm. The lowest

Table 4
The average diameter of the zone of inhibited growth of the examined fungi (mm)[a].

Fungus	Amount of compound (μg)			
	10	20	50	100
1				
A. niger	(36)	(48)	(55)	(62)
A. terreus	(48)	(56)	(66)	(72)
F. oxysporum	(53)	(63)	(70)	(>85)
F. solani	52 (40)	59 (50)	70 (60)	80 (67)
P. ochrochloron	(65)	(75)	(>85)	(>85)
C. tenuis	(23)	(26)	(29)	(34)
2				
A. niger	16	22	28 (10)	(35)
A. tereus	26	(34)	(41)	(47)
F. oxysporum	9	20	30 (26)	36 (32)
P. ochrochloron	(16)	(26)	(34)	(46)
F. solani	0	22	36 (23)	43 (28)
C. tenuis	(20)	(26)	(30)	(36)
3				
A. niger	0	0	8	19 (10)
A. tereus	0	0	12	(13)
F. oxysporum	0	17	23	34 (26)
P. ochrochloron	0	0	12	23 (12)
F. solani	0	n/a	32	45 (24)
C. tenuis	(28)	(32)	(37)	(42)
4				
A. niger	24 (16)	35 (29)	(39)	(46)
A. tereus	20	22	25	(33)
F. oxysporum	17	20	25 (17)	30 (24)
P. ochrochloron	17	32	36	42 (21)
F. solani	n/a	19	n/a	34 (23)
C. tenuis	(20)	(25)	(29)	(33)

[a] Diameter of the zone of the totally inhibited growth of the fungus (no mycelium within the growth medium) is shown in parentheses. The values beyond relate to the diameter of the zone of both: limited and totally inhibited growth of the fungus; n/a – not applicable.

activity toward molds was exhibited by 4-fluoro- substituted benzoxaborole (**3**). This compound limited the growth of fungi in average zone equaled 20–35 mm for the highest tested amount of the boronate. In the case of derivatives substituted with fluorine atom in positions 6 and 7 (compounds **2** and **4**, respectively), the diameter of the zone of limited or inhibited growth was similar and oscillated within 30–47 mm. Opposite to other molds, *C. tenuis* was more sensitive to compound **3** than toward any other from among tested derivatives. This finding makes further search of the influence of the structure of benzoxaboroles on their selective activity against yeasts or filamentous fungi interesting.

3. Conclusions

Molecular and crystal structure of isomers **1** and **2** are very similar. There are also no essential differences in spectral characteristics of all the investigated compounds. The position of fluorine substituent influences the acidity as well as biological activity of the studied benzoxaboroles. The surprisingly low acidity of **4** (pK_a value higher than that of the unsubstituted benzoxaborole) can be explained by the rigidity of the molecule caused by the formation of intramolecular hydrogen bond with fluorine atom. It was previously stated, that higher acidity of substituted benzoxaboroles results in rising of polyols binding properties as well as enzyme inhibition of these compounds [19]. Surprisingly, compound **3** which is the most acidic one amongst the studied isomers, displays the lowest antifungal activity. Lower biological activity was also obtained for this compound against other fungi [17]. Obviously the enzyme-benzoxaborole binding is affected not only by pK_a, influencing formation of the cyclic ester with hydroxyl groups of the enzyme. Another possible factor is the interaction of fluorine atom with the active site of enzyme [29,30]. The fluorine atom in **3** is the most hindered one, which can possibly be the reason of lower antifungal activity of this compound.

4. Experimental

4.1. Synthesis

Compounds **1** was synthesized as described previously [22]. Compounds **2**, **3** and **4** were obtained from the corresponding fluoro-substituted 2-formylphenylboronic acids according to the procedure for **2** described below.

4.1.1. Synthesis of 6-fluoro-2,1-benzoxaborol-1(3H)-ol (**2**)

To stirred solution of 5.05 g (30 mmol) of 4-fluoro-2-formylphenylboronic acid in 180 cm^3 of methanol, 1.26 g of sodium borohydride (33.3 mmol) was added at room temperature in small portions (after addition of whole amount of $NaBH_4$ the color of the solution turned from yellowish to almost colorless). The reaction mixture was stirred for 7 h at room temperature and additional 0.64 g of sodium borohydride (17 mmol) was added at room temperature. The resulting solution was stirred at room temperature overnight and was brought to pH ca. 3 by addition of 3 M aq. HCl at room temperature. Methanol was then removed under vacuum and yellowish suspension was obtained. The suspension was diluted with 25 ml of distilled water and 100 ml of saturated brine was added. Resulting mixture was extracted with 3 × 100 ml of ethyl acetate. The organic layers were combined and the solvent was removed under vacuum, giving 3.03 g of yellowish solid product (66% yield). ^{1}H NMR (500 MHz, methanol-d_4) 7.36 (*m*, 1H), 7.27 (*m*, 1H), 7.18 (*m*, 1H), 5.03 (*s*, 2H); ^{11}B NMR (160.4 MHz, methanol-*d*4) 32.6; ^{13}C NMR (125.7 MHz, methanol-d_4) 164.8, 162.9, 150.7, 124.1 (*d*, *J* = 8 Hz), 119.2 (*d*, *J* = 23.5 Hz), 116.6 (*d*, *J* = 21 Hz), 72.0; single crystals of quality sufficient for X-ray investigation were obtained by two recrystallizations from, in sequence, water and tetrahydrofuran. Compounds **3** and **4** were obtained in similar way in 78% and 54% yield, respectively. It is noteworthy, that above synthetic method gives higher yields compared with those described for these compounds in literature [20].

4.2. X-ray diffraction

A single crystal of suitable size was selected and attached to a cryogenic nylon loop using oil, and mounted on a goniometer head. Determination of the unit cell parameters and integration of raw collected frames were performed with CrysAlis PRO 1.171.36.20 software [32] (supplied by Agilent Technologies). The measurement of diffractional data was performed on a Kuma KM4CCD κ-axis diffractometer with graphite-monochromated Mo Kα radiation equipped with an Oxford Cryosystems nitrogen gas-flow apparatus. Collected reflections were corrected for Lorentz and polarization effects. Multi-scan absorption correction was applied. Data reduction, scaling, merging and analysis of collected data were carried out with the CrysAlis PRO 1.171.36.20 software [32]. The structure was solved by direct methods [33] and refined using SHELXL-97 [34,35] program supported by Olex2 1.2 software [36] (SHELXS-97 was used for direct methods solving). The refinement was based on F^2 against all reflections. Weighted *R* factors, *wR* and all goodness-of-fit *S* values are based on F^2. Conventional *R* factors are based on *F* with *F* set to zero for negative F^2. The $F_O{}^2 > 2\sigma(F_O{}^2)$ criterion was used only for calculating *R* factors and is not relevant to the choice of reflections for the refinement. The *R* factors based on F^2 are about twice as large as those based on *F*. Scattering factors were taken from *International Tables for Crystallography* [37]. Hydrogen atoms were located with use of independent (from difference Fourier maps) refinement, and were refined isotropically. Non-hydrogen atoms were refined anisotropically. Molecular graphics and crystal packing diagrams were prepared with Mercury CSD 3.0 [38] and ORTEP III for Windows [39] software. Hirshfeld surfaces and corresponding fingerprint plots were calculated and visualized with CrystalExplorer 3.0 RC1 software [40].

4.3. NMR measurements

All spectra were recorded at 298 K. The samples concentration was 0.01 M. The ^{1}H, ^{13}C and ^{17}O NMR measurements were performed on Agilent DD2 800 spectrometer, operating at frequencies 799.926, 201.162 and 108.442 MHz, respectively. ^{17}O NMR spectra were recorded using a 5 mm probehead (BB/^{1}H; 90° ^{17}O pulse width 8 μs) using a simple one-pulse sequence (*s2pul*) with increased receiver gating time following pulse (*rof2* = 30 μs) to reduce distortion of baseline. ^{1}H and ^{13}C spectra were acquired using ^{1}H{^{13}C/^{15}N} triple resonance probe (90° pulse width: ^{1}H – 13.6; ^{13}C – 6.9) and standard one-pulse sequence (*s2pul*). The ^{13}C NMR spectra were recorded with broadband ^{1}H decoupling. Line broadening factor of 10 Hz was used for ^{17}O NMR spectra and 1 Hz for ^{13}C spectra. The ^{19}F NMR spectra were recorded on Bruker Avance II 400 equipped with ATM BBO BB(F)/^{1}H 5 mm probehead, operating at frequency 376.498 MHz. Standard one-pulse sequence (*zg30*) and acquisition parameters were used. For measurements of coupling constants, increased digital resolution of ^{1}H, ^{13}C and ^{19}F NMR spectra was needed. It was achieved by using of gaussian multiplication.

4.4. pK_a determination

The value has been determined by a UV–Vis spectroscopy, according to the slightly modified method of Tomsho et al. [19,26]. The details are collected in Supplementary material.

4.5. Biological activity

Czapek medium and YPD medium components of the highest available purity and DMSO were obtained from POCH (Gliwice, Poland). Medium Potato Dextrose Agar and Tween 80 were purchased from Sigma–Aldrich (Poznań, Poland).

Seven fungal strains were used for the experiments. *A. niger LOCK 0440*, *A. pergillus terreus LOCK 64* and *F. oxysporum E95* were purchased from Institute of Fermentation Technology and Microbiology (Technical University of Lodz), while *F. solani* F-454, and *P. ochrochloron* F-337 were obtained from Czech Collection of Microorganism (CCM). *Fusarium dimerum* DAE-1001, originally isolated from the surface of carrot seeds, was taken from the collection of microorganisms of Department of Analytical and Ecological Chemistry (Faculty of Chemistry, Opole University). Yeasts *C. tenuis* DSM-26797 were purchased from Leibniz-Institute DSMZ-German Collection of Microorganisms and Cell Cultures. *Aspergillus* and *Penicillium* strains were routinely maintained in potato dextrose agar while *Fusarium* strains grew in Czapek agar medium. *C. tenuis* was maintained in standard YPD agar medium. In the case of filamentous fungi, spore suspensions used in our experiments as inocula were prepared by washing the surface of 10-14-day-old cultures with sterile 0.05% Tween solution in distilled (Milipore Q) water. Such inocula were then quantified using the Thom's chamber. In the case of *C. tenuis*, two days old cultures of yeasts were used directly for inoculation.

Antifungal activity of boronic compounds has been studied by diffusion agar method [6]. The 0.5 ml of inoculum containing 10^6–10^7 spores or cells was spread on the surface of solidified Czapek, potato dextrose or YPD medium and allowed to dry. The amounts of 100, 50, 25, 10, 5, 2.5 and 1 mg of the tested compounds dissolved in DMSO were placed in 2 mm diameter holes, which were cut in media. A holes in control cultures were filled with DMSO. The duration of incubation of the fungi was dependent on the vigor of their growth and was established as 48 h for *C. tenuis* and *Aspergillus* strains and 72 h for other examined fungi. The optimal temperature for the incubation was 27 °C for *Candida* and *Fusarium* strains and 30 °C for other strains. Each experiment, including control, was carried out in at least three repetitions. Antifungal activity was evaluated by the diameter of the clear zone surrounding the holes, whereas a halo indicated partial inhibition of growth.

Acknowledgment

L. Popenda acknowledges the support of the National Centre for Research and Development under research Grant number 178479, contract number PBS1/A9/13/2012.

Appendix A. Supplementary material

CCDC-1027467 for compound **2** contains the supplementary crystallographic data for this paper. These data can be obtained free of charge from The Cambridge Crystallographic Data Centre via www.ccdc.cam.ac.uk/data_request/cif.

Supplementary data associated with this article can be found, in the online version, at http://dx.doi.org/10.1016/j.bioorg.2015.05.004. These data include MOL files and InChiKeys of the most important compounds described in this article.

References

[1] V.M. Dembitsky, A.A.A.A. Quntar, M. Srebnik, Chem. Rev. 111 (2011) 209.
[2] J.I. Jay, B.E. Lai, D.G. Myszka, A. Mahalingam, K. Langheinrich, D.F. Katz, P.F. Kiser, Mol. Pharm. 7 (2010) 116.
[3] A. Mahalingam, A.R. Geonnotti, J. Balzarini, P.F. Kiser, Mol. Pharm. 8 (2011) 2465.
[4] J.N. Cambre, B.S. Sumerlin, Polymer 52 (2011) 4631.
[5] R.T. Jacobs, J.J. Plattner, M. Keenan, Curr. Opin. Infect. Dis. 24 (2011) 586.
[6] A. Adamczyk-Woźniak, O. Komarovska-Porokhnyavets, B. Misterkiewicz, V.P. Novikov, A. Sporzyński, Appl. Organometal. Chem. 26 (2012) 390.
[7] D. Wieczorek, J. Lipok, K.M. Borys, A. Adamczyk-Woźniak, A. Sporzyński, Appl. Organometal. Chem. 28 (2014) 347.
[8] G.A. Ellis, M.J. Palte, R.T. Raines, J. Am. Chem. Soc. 134 (2012) 3631.
[9] C.T. Liu, J.W. Tomsho, S.J. Benkovic, Bioorg. Med. Chem. 22 (2014) 4462.
[10] www.anacor.com/an2690.php (release 28.01.15).
[11] F.L. Rock, W. Mao, A. Yaremchuk, M. Tukalo, T. Crepin, H. Zhou, Y.-K. Zhang, V. Hernandez, T. Akama, S.J. Baker, J.J. Plattner, L. Shapiro, S.A. Martinis, S.J. Benkovic, S. Cusack, M.R.K. Alley, Science 316 (2007) 1759.
[12] Y.-K. Zhang, J.J. Plattner, Y.R. Freund, E.E. Easom, Y. Zhou, L. Ye, H. Zhou, D. Waterson, F.-J. Gamo, L.M. Sanz, M. Ge, Z. Li, L. Li, H. Wange, H. Cui, Bioorg. Med. Chem. Lett. 22 (2012) 1299.
[13] A. Adamczyk-Woźniak, M. Jakubczyk, A. Sporzyński, G. Żukowska, Inorg. Chem. Commun. 14 (2011) 1753.
[14] A. Adamczyk-Woźniak, M. Jakubczyk, P. Jankowski, A. Sporzyński, P. Urbański, J. Phys. Org. Chem. 26 (2013) 415.
[15] I.D. Madura, K. Czerwińska, M. Jakubczyk, A. Pawełko, A. Adamczyk-Woźniak, A. Sporzyński, Cryst. Growth Des. 13 (2013) 5344.
[16] I.D. Madura, K. Czerwińska, Cryst. Growth Des. 14 (2014) 5912.
[17] M.K. Cyrański, A. Jezierska, P. Klimentowska, J.J. Panek, A. Sporzyński, J. Phys. Org. Chem. 21 (2008) 472.
[18] B. Gierczyk, M. Kaźmierczak, Ł. Popenda, A. Sporzyński, G. Schroeder, S. Jurga, Magn. Reson. Chem. 52 (2014) 202.
[19] J.W. Tomsho, A. Pal, D.G. Hall, S.J. Benkovic, A.C.S. Med. Chem. Lett. 3 (2012) 48.
[20] S.J. Baker, Y.-K. Zhang, T. Akama, A. Lau, H. Zhou, V. Hernandez, W. Mao, M.R.K. Alley, V. Sanders, J.J. Plattner, J. Med. Chem. 49 (2006) 4447.
[21] S.J. Baker, J.W. Tomsho, S.J. Benkovic, Chem. Soc. Rev. 40 (2011) 4279.
[22] I.D. Madura, A. Adamczyk-Woźniak, M. Jakubczyk, A. Sporzyński, Acta Cryst. E 67 (2011) o414.
[23] S. Sene, D. Berthomieu, B. Donnadieu, S. Richeter, J. Vezzani, D. Granier, S. Bégu, H. Mutin, C. Gervais, D. Laurencin, CrystEngComm 16 (2014) 4999.
[24] F.H. Allen, R. Taylor, Chem. Commun. 7 (2005) 5135.
[25] J.J. McKinnon, M.A. Spackman, A.S. Mitchell, Acta Cryst. B 60 (2004) 627.
[26] M.A. Spackman, D. Jayatilaka, CrystEngComm 11 (2009) 19.
[27] M.A. Spackman, J.J. McKinnon, CrystEngComm 4 (2002) 378.
[28] A. Adamczyk-Woźniak, K.M. Borys, I.D. Madura, A. Pawełko, E. Tomecka, K. Żukowski, New J. Chem. 37 (2013) 188.
[29] D. Zarzeczańska, T. Ossowski, A. Sporzyński, unpublished results.
[30] Boronic Acids. Preparation and Applications in Organic Synthesis, Medicine and Materials, in: D.G. Hall (Ed.), Wiley-VCH, Weinheim, 2011, pp. 9–12.
[31] B. Gierczyk, M. Kaźmierczak, G. Schroeder, A. Sporzyński, New J. Chem. 1056 (2013) 37.
[32] O.V. Dolomanov, L.J. Bourhis, R.J. Gildea, J.A.K. Howard, H. Puschmann, J. Appl. Cryst. 42 (2009) 339.
[33] G.M. Sheldrick, Acta Cryst. A 46 (1990) 467.
[34] G.M. Sheldrick, SHELXL93: program for the refinement of crystal structures, Univ. of Göttingen.
[35] G.M. Sheldrick, Acta Cryst. A 64 (2008) 112.
[36] CrysAlis CCD/CrysAlis RED, 171.33.66, Oxford Diffraction Ltd., 2007.
[37] A.J.C. Wilson (Ed.), International Tables for Crystallography, vol. C, Kluwer, Dordrecht, 1992.
[38] C.F. Macrae, I.J. Bruno, J.A. Chisholm, P.R. Edgington, P. McCabe, E. Pidcock, L. Rodriguez-Monge, R. Taylor, J. van de Streek, P.A. Wood, J. Appl. Cryst. 41 (2008) 466.
[39] L.J. Farrugia, J. Appl. Cryst. 30 (1997) 565.
[40] S.K. Wolff, D.J. Grimwood, J.J. McKinnon, M.J. Turner, D. Jayatilaka, M.A. Spackman, Crystal Explorer (Version 3.0), Univ. of Western, Australia, 2012.